CONF-790615--11

MASTER

STRUCTURAL ANALYSIS OF THE UPPER INTERNALS STRUCTURE FOR THE CLINCH RIVER BREEDER REACTOR PLANT

J. L. Houtman

Member, ASME
Westinghouse Electric Corporation
Advanced Reactors Division
Madison, Pennsylvania

ABSTRACT

The Upper Internals Structure (UIS) of the Clinch River Breeder Reactor Plant (CRBRP) provides control of core outlet flow to prevent severe thermal transients from occuring at the reactor vessel and primary heat transport outlet piping, provides instrumentation to monitor core performance, provides support for the control rod drivelines, and provides secondary holddown of the core. The UIS is designed for a sodium environment with temperatures up to 1200°F, transient ramp rates up to 100°F per second, transient temperature changes of as much as 400°F, and as many as 10^9 cycles of normal operation temperature fluctuations of up to 300°F. It is designed to survive these conditions in combination with flow-induced vibration and seismic loadings for a 30 year design life.

All of the structural analysis aspects of assuring that the UIS is structurally adequate are presented in this paper including simplified and rigorous inelastic analysis methods, elevated temperature criteria, environmental effects on material properties, design techniques, and manufacturing constraints.

INTRODUCTION

The conflicting requirements of designing the Upper Internals Structure (UIS) of the Clinch River Breeder Reactor Plant (CRBRP) to survive a severe thermal environment and simultaneously to minimize stress and deflection in the event of an earthquake have resulted in innovative design techniques and design analysis methods. The structural analysis of the UIS has provided the justification and demonstrated the necessity for these design techniques and methods and has also provided the verification of structural adequacy by rigorous analysis.

This paper presents an overview of the structural analysis that has been required for the UIS. The overview naturally begins with a description of the component's requirements, loading conditions, and structural criteria to be satisfied. The design techniques adopted and simplified analysis methods used in sizing the structure are then developed. This is followed by a presentation of a number of the unique design problems that were solved. The rigorous analysis approach, some of the finite element models used, and key results of these analyses are presented in the final part of the paper and are followed by several conclusions and recommendations that are a result of the UIS design analysis effort.

It is intended throughout the paper to reflect the multidisciplined nature of demonstrating structural adequacy. The structural aspects are in themselves

complex and difficult, but it should be recognized that the design, manufacturing, materials, and thermal/hydraulic disciplines are equally so. The successful completion of the UIS design for CRBRP is a result of the team effort of engineers from each of these disciplines.

COMPONENT DESIGN AND REQUIREMENTS

The UIS design configuration is shown schematically in Figure 1. The basic structure is a Type 316 stainless steel weldment that is supported by and constructed around four columns. Four jacking mechanisms are mounted to the closure head and attached to the UIS columns. The lower structure consists primarily of an upper and a lower support plate welded to four shear webs that greatly enhance lateral stiffness since they are also welded to the four columns that extend to the lower support plate. The skirt of the UIS extends downward from the lower support plate forming the mixing chamber and providing the attachment surfaces for the three keys. The keys are equally spaced (120° apart) and insert into the core former structure to minimize vibration during normal operation and minimize deflection under seismic excitation. During refueling, the jacking mechanisms raise the UIS and disengage the keys so that the UIS may be rotated to various positions for inserting and removing core assemblies through the IVTM port. The IVTM Port Plug is in position during normal operation.

Thermocouples are positioned over most of the core assemblies by the instrumentation posts that are shrink-fitted into the lower support plate. The instrumentation posts have one to three fins which contain the Inconel 718 thermocouple dry wells and also cover each of the fuel and blanket assemblies preventing them from ratchetting upward an excessive distance. The center post of the instrumentation post is stainless steel as is the lower support plate into which it fits. Covering this is the Inconel 718 lower section that has the fins. The instrumentation leads are routed from the post positions through conduits to the support columns, up the inside of the columns, and out through the jacking mechanisms.

The UIS chimney assemblies are Inconel 718, mechanically attached with a breech-lock feature to the lower support plate, and are guided by the upper support plate allowing for axial expansion. The Control Rod Drivelines are protected from fast flowing sodium and given lateral positioning by the upper and lower shroud tubes which are also Inconel 718. The lower shroud tubes are mechanically attached to the chimney assembly while the upper shroud tube is supported at the head and slips over the lower shroud tube. The chimneys channel the flow of core effluent from the mixing chamber to the upper part of the outlet plenum promoting additional mixing in the outlet plenum to mitigate transient effects at the vessel outlet and in the hot leg piping. The lower shroud tubes also limit the upward distance that a control assembly may move.

Several thermal liners are provided for protection of the base weldment. Type 316 stainless steel liners are used to mitigate upset and emergency transient effects while Inconel 718 is used in regions where high cycle, steady state temperature fluctuations from mixing will occur. This thermal effect is termed "striping" in CRBRP and will be discussed more fully in later sections. Inconel 718 liner protection has been provided in the mixing chamber, and on the bottom of the skirt for this reason. The material of construction for the chimney assemblies, the lower shroud tubes, and the lower section of the instrumentation posts is Inconel 718 for the same reason. In the case of the upper shroud tube, Inconel 718 is required for the additional reason that greater creep rupture resistance is needed than is provided by Type 316 stainless steel due to the presence of a high steady state gradient.

The interfaces of the UIS columns and IVTM port plug with the jacking mechanisms and head form the primary pressure boundary and are always at low temperature (< 800°F, 427°C). Therefore, these areas of the UIS are required to satisfy the requirements for ASME Class 1 appurtenances. The in-vessel portion of the UIS performs a core support function and is at elevated temperature (> 800°F, 427°C). Since Subsection NG of Section III does not apply to elevated temperature components and since no elevated temperature code case exists for core support structures, the in-vessel UIS is analyzed as a Class 1 component in accordance with Subsection NB of Section III and Code Case N-47 (1592-10). The Nuclear Systems Materials Handbook, Reference 1, and the ASME Code are the primary sources for material properties. These requirements and material property sources are supplemented by RDT Standards E15-2NB and F9-4, respectively, and by additional CRBRP criteria and guidelines for the treatment of environmental effects and for the computation of cumulative creep/fatigue damage when the state of stress is compressive during hold times between transients.

It is the in-vessel portion of the UIS that is of interest for this paper and further references to the low temperature pressure boundary will not be made.

a) Mechanical Loads and Thermal Environment

ASME Code design condition loads are limited to dead weight and pressure. The dead weight of the UIS is about 100,000 pounds (445,000 N) and the differential pressure from inlet to outlet of the chimney assemblies is 5 psi (34,475 Pa). The design temperature of the UIS is 1220°F (660°C). This is the highest temperature expected at any location on the UIS at any time for normal operating conditions.

for normal conditions in order to ascertain structural integrity with regard to fatigue. When not predictable, the number of cycles shall be taken as 10^{10} cycles.

The UIS shall be designed to accommodate thermal striping during normal operation. Thermal striping is the condition that exists when sodium at different temperatures leaving fuel and blanket assemblies impinges upon the exposed surfaces of the UIS. The UIS surfaces directly exposed to thermal striping are the instrumentation posts, control rod shroud tubes, the internal surfaces of the chimneys, and the UIS mixing chamber. Typical striping temperature peak-to-peak amplitudes at several locations in the UIS are shown in Figure 2. The frequencies of the oscillations vary from 0.5 Hz to 2.0 Hz.

The reactor operating temperature, for long term steady state effects in a cumulative damage analysis, is based on a reactor coolant outlet temperature of 1000°F. UIS temperatures for steady state conditions are illustrated in Figure 3. Chimney assembly normal operating exit temperatures are shown in Figure 4, illustrating the planar temperature profile in the UIS. During refueling operations, which are normal operating conditions, the UIS will be at the refueling temperature of 400°F $\pm$ 50°F. Normal operating temperature transients such as start up and shut down are less severe than the upset and emergency events and are enveloped by them.

The upset mechanical loads on the UIS are the seismic input for the operating basis earthquake (OBE) described in terms of response spectra. The response spectrum of the Intermediate Rotating Plug (IRP) and Core Barrel (CB) interfaces with the UIS are obtained from linear time history analysis of

the reactor vessel system using time history input at the vessel support. The UIS may be in the operating configuration, preparation for refueling configuration (keys still engaged), or in the refueling configuration when the operating basis earthquake occurs. Therefore, these three load cases must be considered. In addition to the earthquake response spectra loading, a relative horizontal displacement of 0.37 inch (0.94 cm) between the head and the core barrel must be considered in the OBE seismic response spectrum analysis of the UIS during operation. The UIS must be designed for five OBE events of 10 maximum response cycles each. During refueling the UIS may be positioned in close proximity to the vessel thermal liner. Impact between the UIS and the liner during an OBE is not permitted. The gap at that position is 2.00 inches (5.08 cm).

For the areas of the lower plate, upper shroud tube and column/top plate joint, the most severe upset (U) and emergency (E) thermal transients are U-2b, uncontrolled rod withdrawal from full power, and U-18, loss of preferred and alternate preferred power. For the lower shroud tube, the E-16 emergency transient, three loop natural circulation, is also severe. All other UIS transients are grouped with respect to severity under these transients. Local areas of the UIS are analyzed based on one or more of these transients. These transients are plotted in Figure 5 for an average fuel assembly exit. The fluid temperature changes are less severe farther from the fuel exit as a result of mixing with control assembly flow and blanket assembly flow. These other assemblies also have less severe changes occuring at their exits. The heat transfer analyses of different areas of the UIS account for all of these differences.

The UIS must be designed to accommodate loads due to loss of primary holddown (hydraulic balance) of core assemblies. Loss of hydraulic balance is classified as an emergency event that occurs five times, but it shall be analyzed as an upset event because inspection of the UIS is not planned. The load application due to loss of hydraulic balance is considered to be a gradual process in which random core assemblies move upward and contact the UIS. Consequently, the maximum upward loads on the UIS shall be 95,080 pounds (423,000 N) from 198 fuel assemblies, 60,750 pounds (270,230 N) from 150 blanket assemblies, and 10,890 pounds (48,440 N) from 19 control assemblies. These loads are the products of the number of assemblies times the buoyant force plus the product of the area of the inlet nozzles of the assemblies and pressure difference across the assemblies minus the weight of the assembly. Conservatism has been included by assuming that the pressure drop across the radial blanket assemblies is the same as that across the fuel elements.

The UIS must be designed to withstand the effects of a safe shutdown earthquake (SSE). Though the SSE is a faulted condition, to insure safe shutdown, the UIS is designed to satisfy the ASME code criteria for emergency conditions when in the operating configuration and subjected to the SSE faulted condition loads. During refueling, the UIS is required to be designed to meet faulted allowables. Furthermore, the UIS must be designed such that there is no adverse effect on the control rod drivelines which could prevent safe shutdown. The SSE is a single event of 10 cycles.

Seismic input for the SSE is described in terms of response spectra. In addition to the response spectra loading, a relative horizontal displacement of 0.53 inch (1.35 cm) between the head and the core barrel must be considered in the SSE response spectrum analysis of the UIS during operation.

Two faulted events are identified in the UIS faulted duty cycle. Only one occurrence of either of these events is allowed. Faulted events are not considered in cumulative damage calculations since their occurrence terminates reactor functioning after a safe shutdown has been achieved.

b) Additional Properties and Criteria

Due to the frequencies associated with striping and the 30 year design life of the UIS, high cycle design fatigue curves that cover the range of 10^6 to 10^{11} cycles are required for creep/fatigue cumulative damage evaluations. The CRBRP project has adopted the curves shown in Figure 6 for use on the UIS. The Type 316 stainless steel fatigue curve is an extrapolation of the Code Case N-47 at 1000°F to 1200°F (538°C to 649°C) from 10^6 cycles using a slope on cycles of -0.12. This is based on the slope of the elastic term of the Universal Slopes Equation of Reference 2. The Inconel 718 fatigue curves for varying amounts of mean stress are from Reference 3.

The CRBRP project has also adopted an exception to the cumulative creep/fatigue damage rule of Code Case N-47 and RDT Standard F9-4. Since the in-vessel UIS is not a Class 1 component and is not a Code Component, a relaxation of the rule for compressive sustained stress situations was considered permissible knowing that hold-time fatigue tests of stainless steel with compressive hold periods reflect similar life capabilities as continuous cycling tests, Reference 4. The rule adopted assumes that compressive hold, creep rupture damage is 20% as

damaging as the damage caused by the same sustained stress in tension. It applies for austenitic stainless steel (Types 304 and 316) at metal temperatures less than 1200°F (649°C), and is subject to the verification that the effective number of expected cycles to failure would be less than 3000 cycles for Type 316 and less than 6000 cycles for Type 304, based on Reference 5. At times in the duty cycle when sustained stresses are tensile, damage is computed in accordance with Code Case N-47. Compression is defined as a stress state where none of the principal stresses are tensile.

c) Environmental Effects on Material Properties

Most of the data used to define the allowable design stresses, stress rupture and fatigue strength in the ASME Code were obtained from mechanical tests conducted in air. Procedures were used to account for scatter, specimen size and finish in the available data so that the design values are adequately conservative. However, no attempt is made by the Code to account for the effects of the service environment. That job is assigned to the designer.

The development of the CRBRP UIS has focused attention on the mechanical behavior of reactor materials when exposed to high-temperature liquid sodium, in addition to fast neutron irradiation and a long time aging at elevated temperatures.

For locations on the UIS where Inconel 718 and 316 SS would receive the highest neutron dosage, the total fluence level should be less than 1.0×10^{21} neutrons/cm^2. Therefore, the effects on mechanical properties should not be significant and are not modified.

Type 316 stainless steel is a non-age hardenable alloy. Thus, no significant changes in strength or hardness of annealed material would accrue from long term aging at temperatures up to 1100°F, unlike the precipitation-hardened stainless steels. Some slight increases in strength and decreases in ductility may occur due to carbide formation, together with a reduction in the room temperature impact strength. In contrast to Type 316 stainless steel, Inconel 718 is an age hardenable alloy. However, the age hardening action (precipitation of a gamma prime type intermetallic compound) is very sluggish. Consequently, when age-hardened material is subjected to aging at temperatures up to 1100°F, no deleterious changes in strength or ductility are likely to be observed. No allowances have been made for the effects of thermal aging on the properties of Type 316 stainless steel and Inconel 718.

At temperatures above 900°F (482°C), the presence of liquid sodium begins to affect the properties of these materials. This occurs through a surface effect and through an interstitial transfer effect. Interstitial transfer of elements such as carbon and nitrogen can occur by a diffusion process. Observed effects on limited data where interstitial transfer has not occurred is termed a surface effect. The only effect of sodium on Inconel 718 that is accounted for is a surface effect on long term stress rupture strength of up to a 10% reduction. This is assumed to be the same as stainless steel out of conservatism. Interstitial effects are accounted for on several properties of 316 SS. Namely, a reduction in yield and ultimate strength of up to 20%, an increase in elongation of up to 30%, and a loss of stress rupture strength of up to 35%. Limited data on fatigue properties of the two materials indicates that a slight increase in fatigue strength due to lack of surface oxidation may occur but no benefit has been permitted.

As a result of the paucity of in-sodium, long-term data for these materials, an extensive mechanical property development test program has been initiated for both Inconel 718 and Types 304 and 316 stainless steel. Tensile, low and high cycle fatigue, stress (creep) rupture, creep/fatigue interaction, and thermal shock data will be obtained to verify or modify the effects being considered.

THE DESIGN APPROACH

The mechanical and thermal loading conditions expected for the UIS represent conflicting requirements in that the mechanical loadings require stiffness and strength (or increased thicknesses) and the thermal conditions result in a need for flexibility and reduced thicknesses. Thermal striping imposes a constraint in that Inconel 718 is required in many areas where high cycles (10^9) of these temperature fluctuations are too severe for stainless steel. Additional constraints are imposed because of manufacturing considerations. These include the fact that an all Inconel 718 structure is not possible using commercial heats on a large scale because of welding limitations and that a thin (< one inch thick) stainless steel structure would experience unacceptable distortion during welding. From a structural adequacy viewpoint, neither bimetallic welds nor threaded fasteners would be able to meet the service life requirements and these are therefore not permitted.

These conflicting requirements and various constraints helped to formulate the design philosophy that led to the UIS configuration. A strong and adequately stiff stainless steel weldment with relatively uniform thermal inertia was required. It would utilize stainless steel thermal liner protection for joints and unavoidable heavy sections (> one inch) in hotter regions. It would utilize Inconel 718 liner protection to withstand striping. It would minimize abrupt thickness changes. And all liners would be attached mechanically without threaded fasteners. Stiffness would be achieved through the use of a shear web and by keying the UIS to the core former structure.

Proper selection of thicknesses for the stainless steel base metal and liners and the proper location of Inconel 718 liners were key considerations. To approximately determine the areas that would require Inconel 718, allowable stream-to-stream fluid temperatures were developed as a function of required cycles for a sinusoidal fluid temperature change. The metal temperature differences and stress responses were obtained varying film coefficients and frequencies. Figure 7 illustrates the results obtained for both Inconel 718 and 316 SS. For 22.5 full power years and a 1 Hz frequency, the required number of cycles is 7.1×10^8 cycles. At this frequency, the stream-to-stream fluid temperature allowable of 316 SS is about 50°F (28°C) for a film coefficient of 5000 BTU/hr-ft^2-°F (28,392 W/m^2-°C), while for Inconel 718 with a $\sigma_{max} \leq 64{,}000$ psi (4.41×10^8 Pa), it is about 220°F (122°C) for a film coefficient of 20,000 BTU/hr-ft^2-°F (113,569 W/m^2-°C). Lower film coefficients would of course give higher allowables. Higher maximum stresses, on the other hand, would give lower allowables for Inconel 718. These higher maximum stresses must consider stresses from fabrication as well as applied stresses. Thus, the fabrication process is very important for Inconel 718 since residual stresses can vary significantly. The fabrication processes for the UIS are carefully controlled to assure that residual stresses are as low as possible.

Selection of approximate thicknesses for the 316 SS base metal and liners required the development of a simplified inelastic analysis method and creep/fatigue damage method. Figure 8 shows creep damage for 316 SS in sodium as a function of temperature for increasing compressive hold stress. At a creep damage of 1.0 in the temperature range of 1050°F (566°C) to 1100°F (593°C), considerably less than the minimum yield stress is permissible for

the hold-times between transients. Therefore, the elastic method of Code Case N-47 would indicate that the UIS can not be used in its anticipated environment since it requires the use of 1.25 times the minimum yield strength when the elastically calculated range of primary-plus-secondary stress is large by comparison.

The methods of References 6 and 7 were developed to obtain the approximate elastic-plastic strain ranges (using elastic analysis) from thermal transients acting on simple geometries. Knowing the approximate elastic-plastic strain range $\Delta\varepsilon$, fatigue damage may be computed using the design fatigue curve for inelastic analysis of Code Case N-47. The strain range $\Delta\varepsilon$ also forms the basis for a simplified approach to obtain the residual stress after the transient decays.

The initial residual stress that occurs immediately upon decaying of a transient is obtained with the bilinear construction shown in Figure 9. The loading portion of the cycle is represented by the monotonic, bilinear stress-strain curve as modified by the sodium effects factor K_N. The unload portion of the cycle is obtained using the tenth cycle hardening stress-strain curve obtained through the use of the hardening factor K_c and the sodium effects factor K_N. The initial residual stress is:

$$S_R = S_D - K_N K_c \Delta S \qquad (1)$$

where:

$$S_D = K_N S^L_{max} - (K_N S_{IL} + K_N K_c S_{IU})$$

$$\Delta S = S^U_{max} - S_{IU}$$

The "L" (or load) stresses are obtained from the monotonic stress-strain curve at the load temperature (at peak strain) while the "U" (or unload) stresses are obtained from the monotonic stress-strain curve at the unload temperature. The slope of the plastic portion of the bilinear stress-strain curves is obtained by a straight line through the stress-strain points on the monotonic stress-strain curve at strains of $\Delta\varepsilon$ and $\Delta\varepsilon/2$.

The sodium effects factor K_N is obtained from the expression

$$K_N = \frac{\sigma_y\ (C+N)_e}{\sigma_y (C+N)_o} \qquad (2)$$

where from Reference (8),

$$\sigma_y(C+N) = \begin{cases} \text{[304 Stainless Steel]} \\ 89952 + 181167\ (C+N) - 82T(C+N) \\ -4269T^{1/2} + 58T \\ \text{[316 Stainless Steel]} \\ 88474 + 211640\ (C+N) - 114T(C+N) \\ -4295T^{1/2} + 62T \end{cases}$$

T = temperature, °R

RDT Standard F9-4T suggests the use of the guidelines for inelastic analysis contained in RDT Standard F9-5T. The procedure presented here follows those recommendations in that it utilizes a bilinear representation of the stress-strain curve and accounts for the cyclic hardening behavior of austenitic stainless steel through the application of the tenth cycle stress-strain curve. In using the bilinear representation for the monotonic curve and the tenth-cycle curve in an analysis, the size of the initial yield surface is determined by κ_0.

$$\kappa_0 = \frac{1}{3}\sigma_{Yo}^2$$

where σ_{Yo} is the intersection of the plastic and elastic lines of the monotonic, bilinear stress-strain curve. The size of the yield surface for the first reversed plastic loading and for all subsequent plastic loadings is determined by κ_1.

$$\kappa_1 = \frac{1}{3}\sigma_{Y1}^2$$

where σ_{Y1} is the intersection of the plastic and elastic lines of the plastic and elastic lines of the tenth cycle, bilinear stress-strain curve. Thus, the cyclic hardening factor is:

$$K_c = \frac{S_{Y1}}{S_{Yo}} = \left(\frac{\kappa_1}{\kappa_o}\right)^{1/2}$$

The data of Reference (1) have been utilized to determine that

$$K_c = \left(\frac{\kappa_1}{\kappa_o}\right)^{1/2} = [-0.114 + 3.094\ \Delta\varepsilon]^{1/2} \qquad (3)$$

(for $\Delta\varepsilon \geq 0.36\%$) is a slightly conservative expression for use with both types 304 and 316 stainless steel.

The creep damage is based upon the sustained residual stress during the hold-time between transients. The residual stress resulting from a thermal transient will relax (reduce) during the hold-time in accordance with the creep rate equation for the material. In the simplified approach used on the UIS, the uniaxial expression

$$\frac{1}{E}\frac{d\sigma}{dt} + \dot{\tilde{\varepsilon}}(\sigma) = 0 \qquad (4)$$

was used to simulate the material behavior. To obtain the time to rupture for a given stress, the stress must be divided by K' (=0.9) to comply with Code Case

N-47. In addition, the effect of carbon and nitrogen depletion is accounted for by dividing by the factor F_N where

$$F_N = F_I \, F_S \tag{5}$$

and

F_I = Interstitial Effect (304 and 316 Stainless Steel)

$= 1.0-[(C + N)_o - (C + N)_e] \, [-6.476 + .00848F]$

F_S = Surface Effect (304 and 316 Stainless Steel)

$= 1.2745 - .000305F$

F = temperature, °F

The carbon and nitrogen equilibrium content is obtained from Reference (1) using a carbon potential of 50 ppm for CRBRP. The initial content is assumed to be 0.12% based upon the chemistry of typical stainless steels.

The simplified damage evaluation method may be used to a) evaluate a single type of thermal transient event, b) compare the severity of different thermal transients, c) evaluate the total damage from a duty cycle, and d) establish acceptable thicknesses of liner protection or thicknesses of base metal that would not need liner protection. Figures 10 and 11 illustrate the damage versus thickness information that was generated for the UIS. The basic assumption for these figures is that the duty cycle is simplified to be 577 cycles of the U-2b transient for 22.5 full power years, and that the U-2b temperature versus time is the same for each case, after the initial time.

The variation of damage with thickness of an unprotected section is shown in Figure 10. The steady state, or hold-time temperature T_o, is varied to give three curves, one for 1000°F (538°C), 1050°F (566°C), and 1100°F (593°C). The results indicate that for a T_o of 1000°F (538°C), there would be no limitation

on thickness for an unprotected section up to about 4.0 inches (10.2 cm). However, when the hold-time temperature reaches 1050°F (566°C) and above, severe manufacturing restrictions may result since the thicknesses must be limited to less than about 0.5 inch (1.27 cm) to get the creep/fatigue damage below 1.0.

Figure 11 shows the effect that varying thicknesses of liner protection has on the creep/fatigue damage of a 1.5 inch (3.8 cm) thick base metal section at a T_o of 1100°F (593°C). Again to obtain a damage level less than 1.0, liner protection of about 0.9 inch (2.3 cm) is required. Going back to the T_o = 1100°F (593°C) curve of Figure 10, the 0.9 inch (2.3 cm) liner protection must be provided by a stackup of liners that have a limitation of about 0.2 inch (0.5 cm) for the outside liner. These two figures illustrate one of the fundamental problems faced in the design of the UIS.

The success of the simplified inelastic analysis and creep/fatigue damage method was recognized to be dependent upon the absence of structural ratcheting. Fortunately in this regard, no sustained mechanical loadings of any significance would be applied to the UIS. The largest mechanical loads would come from earthquakes. These loadings are transient and in meeting primary limits at critical bending locations such as the columns, stresses throughout most of the UIS are considerably less than the yield strength. The other consideration would be elastic follow-up or sustained secondary stress from thermal gradients. Therefore, significant consideration was given to the reduction of steady-state secondary stresses and to balancing the stiffnesses of the structure in the hotter regions where ratcheting would more easily occur.

SPECIAL DESIGN PROBLEMS

By referring again to Figure 8, the sensitivity of the 316 SS structure's creep/fatigue damage (with sodium effects) to hold-time temperature for a constant stress is evident. A change in steady-state operating temperature of 10°F (5.6°C) could easily result in a 50% change in the predicted creep damage. Similarly, a 2000 psi (1.38×10^7 Pa) change in residual stress can do the same thing. Thus, slight revisions in predicted operating temperatures or seemingly minor changes in a design to reduce the cost of fabrication can result in a major impact on structural adequacy. On the other hand minor changes in one or the other has solved problems in being able to demonstrate adequacy.

The lower plate of the UIS and its ligaments were the most difficult to design due to their presence immediately above the core and their interaction with the entire struture. Mixing of core and blanket assembly effluents below it, the passage of those flows through the chimney holes, and the slow circulation of cooler, more uniform temperature fluid above results in a complex three-dimensional temperature distribution during both normal operation and transient conditions. In the preliminary design phase, analysis indicated that the plate would not experience a steady-state axial temperature gradient, that the plate radial gradient at steady state would be 60°F (33°C), and that the long term plate temperature at the critical ligament would be 1084°F (584°C) in the chimney hole. These conditions resulted from a conclusion that the trapped sodium above the plate and inside the shear web would be fairly stagnant and from the presence of outlet flow modules that provided 4.5 inches (11.4 cm) of Inconel

718 liner protection on the bottom surface. Therefore, the sizing of required liners by the simplified methods was successful and confirmed by more rigorous analysis, which also showed that stresses in the plate due to its interaction with the remaining structure were low. Subsequent to that time, the chimney hole pattern was revised, the outlet flow modules were eliminated, and thermal/hydraulic test data became available for the UIS. The revision of the hole pattern consisted of the number of chimney holes being reduced in the lower plate and made to be the same size to reduce fabrication costs. The revised pattern, however, left significant regions of solid metal where chimney holes had previously been located. The outlet flow modules were eliminated because of severe flow-induced vibration. These were replaced with instrumentation posts to position the instrumentation over the core assemblies and provide secondary hold-down for the core. Liners were also added to the bottom surface of the plate to protect it from striping and transients. The total thickness of the one Inconel 718 and three 316 SS liners was 1.25 inches (3.18 cm) instead of the previous 4.5 inches (11.4 cm). Thermal/hydraulic tests followed and provided data that indicated that the lower plate would have an 84°F (46.7°C) steady-state axial gradient, a 100°F (55.6°C) steady-state radial gradient, and a long term temperature on the lower surface of the critical ligament of 1105°F (596°C). Revised rigorous analysis predicted excessive creep/fatigue damage.

Early attempts to improve the design by using the simplified inelastic approaches were unsuccessful. This was due to the fact that the elastically calculated stresses that are the basis of the method were not accurately predicted for the ligament and that the elastic-plastic strain corrections were too low. Refining the accuracy of the temperature gradients predicted in the ligament and separating the plate interaction stresses from the through-thickness gradient stresses revealed the solution for the design.

Essentially, the conditions of the preliminary design lower plate had to be duplicated. Two more inches (5.08 cm) of liner protection was obtained by reducing the plate thickness from 6.0 inches (15.2 cm) to 4.0 inches (10.2 cm). The total liner protection provided would be 3.25 inches (8.3 cm) for the bottom of the new lower plate. The three dimensional refined temperature solution for the ligament showed that response of most of the ligament would then be mostly through-thickness response from the chimney holes. The simplified method was then used to increase the chimney assembly thickness in the chimney hole to an acceptable thickness of 1.1 inches (2.8 cm) from 0.75 inch (1.9 cm). The long term temperature at the bottom corner of the ligament had also been reduced to 1088°F (587°C) and the steady-state axial gradient to 60°F (33°C). Three inch diameter blind holes were added to the solid portion of the lower plate. In addition to reducing the stiffness of this region to be balanced with the stiffness of the chimney hole area, this permitted metal temperature response of nearly the entire plate to be very uniform during transients. Detailed elastic analysis shows that this restricted the in-plane membrane stresses in the critical ligament (from interaction with the rest of the structure) to fluctuate only 5000 psi (3.44×10^7 Pa) during the U-2b transient. The steady-state membrane stress had also been reduced by 2000 psi (1.38×10^7 Pa). Rigorous analysis confirmed the acceptability of the design.

The use of Inconel 718 in regions of large striping amplitudes was initially thought to be free of complications. Examples of problems that were foreseen were the effects of grain size and mean stress on the fatigue endurance. Available data supported the need for fabrication control to minimize residual stresses. Grain size control was considered to be impractical and the design was able to accommodate the possibility of larger grains. An unforeseen problem

surfaced when operating conditions on the lower shroud tubes where shown by test data from different tests to either have lower striping amplitudes and large steady-state gradients, or to have higher striping amplitudes with moderate steady-state gradients. The striping fluid temperature range could be as high as 163°F (91°C) and the steady-state gradient could be 358°F (199°C). Uncertainties in the data and with the flow needs of the interfacing Control Rod Driveline led the designer to opt for a design that would satisfy both conditions.

The limitation that surfaced in the evaluation of the lower shroud tube is in the fact that Inconel 718 stress rupture properties become limiting even though stresses are well below the yield strength, Reference (1). Another limitation that was recognized was the combined effect of fabrication residual stresses with applied mean stress on the fatigue endurance. With a 163°F (91°C) fluid striping range, the steady-state gradient would have to be less than 200°F (111°C). The design was therefore changed to two concentric Inconel 718 tubes with a gap between them. This limits the potential steady-state gradients to an acceptable level of less than 150°F (83°C) in the outer hot cylinder. Additionally, to accommodate the striping of 163°F (91°C), a maximum cylinder thickness of 0.10 inch (0.25 cm) had to be imposed. At around 0.125 inch (0.32 cm), further reductions in thickness result in the mean temperature following the oscillation in the fluid temperature thereby reducing the temperature gradient and induced surface stress. The 0.10 inch thickness provided adequate reduction in stress amplitude.

OVERVIEW OF THE RIGOROUS ANALYSIS

The structural analysis of the UIS has involved the coordination of many engineering disciplines. Thermal-hydraulics, materials, manufacturing, and design groups all interacted with the structural analysts to assure that the UIS would meet its requirements. Elastic analysis, simplified inelastic and creep-fatigue damage analysis, and finite element inelastic analysis were used as economically as possible to arrive at a detailed design. Ultimate verification of the design was the result of rigorous and detailed finite element elastic and inelastic analysis. Experience and judgement were used to limit the extent of these evaluations as well. The results of these analyses were evaluated against the ASME Code, RDT Standards, and special CRBRP criteria as noted previously. In addition, two structural tests were conducted to support allowables used for buckling of the UIS columns and for stress rupture strength of the 316 SS central rod of the instrumentation posts.

a) Seismic Analysis

In order to evaluate the primary stresses in the UIS due to seismic excitation and to provide detailed seismic stresses to combine with thermal transient results, a response spectrum analysis of a 180 degree finite element model of the structure was performed. The detailed model of Figure 12 simulates the mass and stiffness of the UIS structure including the effects of liquid sodium mass trapped within the structure. Wavefront reduction and other procedures were implemented to allow the large finite element model to be run on the CDC7600 computer. Numerous check runs and static solution runs were performed to evaluate the adequacy of the modeling. Finally, modal analysis of the UIS model for both operating and refueling configurations was performed to obtain natural frequencies and mode shapes. Lowest natural frequencies for the predominant modes of the UIS are, 2.5 hz refueling and 14.3 hz operating.

The seismic analysis was performed with response spectra curves developed for a 0.25g safe shutdown earthquake (SSE) and for a 0.125g operating basis earthquake (OBE) utilizing response spectrum analysis. For each earthquake, the UIS was analyzed for two configurations; refueling and operating. During refueling the UIS keys are disengaged from the core former ring, the IVTM Port Plug is removed, and the UIS is supported only at the intermediate rotating plug. During operation the keys are engaged in the core former ring and the IVTM Port Plug is installed. Stress and displacement results from each mode of the response spectrum analysis are combined by the square root of the sum of the squares for a given excitation direction. Results for each excitation direction, one vertical and two mutually perpendicular horizontal, are also combined by the square root of the sum of the squares. Stresses due to horizontal support point motion and due to dead weight, are added by absolute value to response spectrum analysis stresses to give final values for comparison to criteria.

Primary stress limits are satisfied everywhere in the UIS for the seismic loadings. The lowest margin, however, occurs for a different mode of failure than that protected against by the primary limits. Prevention of buckling, or more specifically plastic instability, of the support columns was the most difficult to justify. The most highly loaded support column is subjected to both axial compression and end moments that cause stresses that are close to the primary stress limits. If a column buckling load is calculated that assumes interaction of the end moments, the required load factors of 3.0 and 2.5 for OBE and SSE during normal operation (SSE is treated as an emergency event) are not satisfied. The UIS column, however, has a D/t of 13.0 which

puts it into the thick cylinder realm, where elastic column buckling would not occur before plastic instability. To verify this and to determine the moment capability of the column, five cylindrical specimens with D/t in the range of 10.0 to 20.0 were collapsed under four point loading. The mode of failure for each was an ovalization of the circular cross-section that led to unstable plastic collapse. A safe instability limit of 0.8 of the minimum ultimate tensile strength was established. Since circumferential wrinkles did not occur, it was also concluded that the end moments on the UIS support columns would not interact with the axial compression to reduce the buckling allowable. Therefore, the load factors for the support columns were satisfied with a uniaxial buckling allowable that accounts for plasticity effects, and the end moments were shown to be less than the moment that would cause a stress of 0.8 of the minimum ultimate tensile strength.

b) Duty Cycle Reduction

The UIS is subjected to a large number of upset and emergency condition thermal transients. Rigorous analysis of each of these events in each of the critical areas of the UIS is impractical from a cost and time standpoint. The purpose of the duty cycle reduction is to reduce the number of events to be applied in the analysis of each area of the structure to only one or two events and to obtain equivalent creep and fatigue damage for the entire duty cycle. This can be achieved by applying an equivalent creep and fatigue damage approach to the umbrella transient events. In a low temperature component where only fatigue damage is involved, this reduction is fairly straight forward since only elastic stress ranges need be determined to enable an equivalent fatigue damage evaluation. In a high temperature component such as the UIS,

time dependent response and environmental effects become governing factors. Residual stress, hold-time between cycles, elastic-plastic strain, cyclic-hardening, and creep/fatigue interaction must all be properly accounted for. The methods of References 6 and 7 and the simplified creep-fatigue damage approach described previously permit this duty cycle reduction to be accomplished in a rapid systematic manner.

The complex nature of the fluid flow distributions in and around the UIS makes it necessary to perform duty cycle reductions at various locations. Steady state operating temperatures, heat transfer coefficients, and transient ramp rates vary from location to location. Together with the thickness variations within the structure, they may cause a range of equivalent cycles that are possible when the duty cycle is reduced to one or two events.

The umbrella transients are grouped into similar categories for reduction by equivalent damage to a single event in that category. That event is the worst event in that category so that the analysis accounts for and identifies the highest level of stress and strain to be experienced by the component. The transients are grouped into the categories of down events, up events, up and down events, and down-up-down events. Having obtained the equivalent number of cycles of the worst event in each category, these are then combined as a duty cycle, if possible, to achieve the fewest different transients that have to be evaluated and the equivalent number of cycles of each to represent the entire duty cycle.

The results of this evaluation for the UIS concluded that the U-2b and U-18 transients (plotted in Figure 5) would have to be treated as separate events for the critical stainless steel areas of the column-top plate joint and the lower plate ligament. The more rapid up transients such as E-16 were determined to have little effect on these well protected areas. It also showed that the number of equivalent cycles could be taken as the total of 577 events without undo conservatism because there is very little creep relaxation of residual stresses during hold times and since the fatigue damages are generally low. However, for unprotected regions such as the liners, the lower shroud tube, and the instrumentation post, the evaluation showed that the E-16 transient would be severe and should also be included in the stress analysis as a separate event.

c) Redundant Thermal Stress Analysis

The basic stainless steel structural weldment of the UIS is a highly redundant structure. Variations in temperature and geometry result in critical regions that are very localized. Calculations or finite element solutions in sufficient detail to accurately assess the stress states in these localized areas are therefore required. Since these areas may not be known a priori and are affected by interaction with other regions of the structure, an overall solution of the structure is also required. Computer storage limitations and cost considerations quickly rule out the possibility of an overall, finely detailed finite element model and solution. Therefore, the UIS thermal stress evaluation of the stainless structure was performed with a series of finite element solutions. These solutions progress from a coarse model of the overall structure, the gross model of Figure 13(a), to one or two more refined models covering

less structure, as illustrated by the lower plate and ligament models of Figure 13(b) and 13(c), respectively. The gross model provides boundary conditions for steady state and transient conditions to the succeeding model which in turn does the same if a third model is involved. As shown in Figure 13 the analysis of the critical ligament in the lower plate required three finite element solutions for steady state and transient conditions. The column-top plate joint utilized two models, while less critical areas such as the shear web, skirt, and lower plate outer ledge were evaluated with the gross model results.

In an elevated temperature design such as the UIS, ratcheting and elastic followup are serious considerations for two reasons. First, the strain levels reached must meet allowables and secondly, the accuracy of detailed solutions by successive solutions depends on it. For example, a choice must be made between using displacement boundaries or force boundaries for the more localized models. The UIS solutions were based on force boundaries because of the ease of interpolation of forces for the finer boundary mesh of the more lozalized model and to avoid the potential problems of localized inaccurate strains and underestimated displacements in going from the coarser mesh to the finer mesh. However, the larger region coarser mesh solutions tend to overestimate forces because of the stiffer representation of the structure and can very easily result in greatly exaggerated strains in the more lozalized and more flexible models (for thermal interactions that are basically secondary effects or displacement controlled). As a result, the design of the lower plate incorporates the features described previously that minimize the interactive forces on the critical ligaments.

The thermal hydraulic analysis of the UIS follows the same succession as the stress analysis and in most cases is more involved at each level to assure that overly conservative interactive forces are not provided to the next solution. Separate local evaluations, for example, were performed for the gross model to provide accurate temperatures for the coarser structural elements in areas such as the column and the upper and lower plates. Considerable effort, therefore, went into interfacing codes which transferred temperatures from one format to another and in averaging and linearizing temperatures to assure that the proper structural effects would be present.

d) Lower Plate and Ligament Analysis

The results of the elastic solution for the UIS gross model for the U-2b and U-18 transients indicates that most of the structure remains elastic and that most of the structure is at a low enough temperature (< 1000°F, 538°C) that creep effects are negligible. Plasticity is indicated in the lower plate and ligaments and ligament temperatures are well into the creep range. Therefore, the forces obtained from the elastic gross model solution are used as boundary conditions for the lower plate model, and the lower plate and ligament solutions are performed inelastically.

The lower plate inelastic thermal stress analysis for the U-2b and U-18 transients was performed on a 180 degree model comprised of flat, triangular shell elements that have membrane and in- and out-of-plane bending capabilities with five temperatures specified through the thickness. It provides nodal forces for the ligament analysis, demonstrates the adequacy of the lower plate to react the loss of hydraulic holddown load, and demonstrates that the plate satisfies the ratcheting criteria. Actually, ratcheting is not a significant

concern from a strain limit standpoint since the strain accumulations during shakedown are in the compressive sense for the highly strained central region of the plate.

The critical ligament was selected on the basis of the most severe transient and steady state temperature conditions since creep-fatigue damage is the most limiting criteria. Symmetry of the thermal environment permitted the use of a half-ligament model with in-plane bending forces being conservatively applied. The model is comprised of 3-D solid elements arranged in seven layers through the depth of the ligament. Thin surface elements are included so that peak strains that account for sodium effects in the stress-strain relations would be obtained. The interaction of the interference fit with the instrumentation posts was accounted for with the use of a solid bar and interfacing gap elements. The stress-strain response of the critical location of the ligament is shown in Figure 14. The resulting creep-fatigue damage satisfies the CRBRP modified damage criteria.

e) Instrumentation Post Analysis

The instrumentation post is a composite structure with a 316 stainless steel central post that is pressfit into the lower plate. Radial pins and a tight fit secure the Inconel 718 outer forging, visible in Figure 1. The Inconel 718 portion is basically a thick cylinder with a tapered end that supports three fins. These fins provide secondary holddown of the core assemblies, support the drywells for the UIS thermocouples, and support the plate liners for the bottom surface of the lower plate and ligaments. This Inconel 718 forging is exposed directly to the fuel and blanket assemblies effluent which subjects

it to striping and transient conditions. Two-dimensional finite element analyses of various sections of the finned cylinder accounted for fillets and holes and utilized temperature boundary conditions based on test data. These solutions demonstrated the adequacy of the part to meet requirements.

An axisymmetric finite element solution was performed for the upper portion of the post. It included both the stainless and Inconel parts and a portion of the lower plate and liners to properly account for the interference fit and simulate the heat transfer effects of the plate. The radial pin holes in the stainless steel portion were not specifically modelled in the axisymmetric representation. At this location a maximum residual compressive stress of an acceptable magnitude (based on code rupture curves) resulted. RDT Standard F9-4T, however, specifically requires the use of peak stress at an area of a stress concentration and retains the requirement of the code to use minimum creep rupture properties. Applying a concentration factor to the peak strain resulted in a residual stress at the hole that gave an unacceptable creep-fatigue damage.

The effects of the presence of stress concentrations on stress rupture properties is known to vary considerably with the material, geometry of the stress concentration, the environment, and life. In the case of the austenitic stainless steels (304, 316, 321 and 347), test data consistently points to stress concentrations having a less severe effect on stress rupture strength than predicted using Code Case N-47 with F9-4T inelastic analysis rules. In the case of 316 SS, there is a consistent trend to significant notch strengthening

for certain notch geometries, particularly when the service environment exceeds 1100°F (593°C) and the time to rupture is long (> 5000 hrs), Reference 8. An existing development test program for in-sodium properties of austenitic stainless steels was modified to include creep rupture and creep-fatigue testing of notched bar (3 transverse holes) samples that simulate the instrumentation post configuration. The results of these tests, Reference 9, clearly indicate strengthening or longer life for both creep rupture and creep-fatigue interaction. The acceptability of the damage calculated on the basis of maximum nominal stress, neglecting the presence of the radial holes, was therefore demonstrated.

CONCLUSIONS AND RECOMMENDATIONS

As a result of the experience gained in designing and analyzing the CRBRP Upper Internals Structure, several conclusions and recommendations can be made that can serve as guidance or as a frame of reference for others involved in the design and analysis of elevated temperature components.

1. A coordinated effort with designer, thermal-hydraulics analyst, and manufacturing engineer must be maintained throughout all design phases of the component.

2. Every effort should be made to get accurate fluid temperatures by analysis or test at the earliest possible time.

3. Simplified inelastic analysis and creep-fatigue damage methods that are approximately accurate (not overly conservative) should be used extensively in the conceptual and preliminary design phases.

4. The design should incorporate features that minimize steady state stresses from mechanical loads, local thermal gradients, or thermal interaction loads.

ACKNOWLEDGEMENTS

The UIS structural evaluation required the concerted effort and skill of many analysts. The author is indebted to those who made a contribution, especially P. T. Falk, M. Kosanchich, Sr., J. M. Thompson, W. W. Webbon, and H. H. Ziada of Westinghouse Advanced Reactors Division, and J. L. Bittner and J. S. Solecki of Swanson Engineering Associates Corporation.

REFERENCES

1. "Nuclear Systems Materials Handbook", TID 26666, Hanford Engineering Development Laboratory.

2. Manson, S.S., "Fatigue: A Complex Subject - Some Simple Approximations," Experimental Mechanics, 5, No. 7, pp. 193-226, July 1965.

3. Jaske, C.E., and O'Donnell, W.J., "Fatigue Design Criteria for Pressure Vessel Alloys," Transactions of the ASME, Journal of Pressure Vessel Technology, Vol. 99, No. 4, pp. 584-592, November 1977.

4. Esztergar, E. P., "Creep-Fatigue Interaction and Cumulative Damage Evaluations for Type 304 Stainless Steel Hold-Time Fatigue Test Program and Review of Multiaxial Fatigue," ORNL-4757, June 1972.

5. Lord, D.C., and Coffin, Jr., L.F., "Low Cycle Fatigue Hold Time Behavior of Cast Rene 80," Metall. Trans. 4, No. 7, pp. 1647-1654 (1973).

6. Houtman, J.L., "Inelastic Strains from Thermal Shock, "Machine Design, Vol. 46, No. 7, pp. 190-194, March 21, 1974.

7. Houtman, J.L., "Elastic-Plastic Strains from Thermal Shock at a Discontinuity - A Simplified Approach," in: Simplified Methods in Pressure Vessel Analysis, PVP-PB-029, pp. 1-14, June 1978.

8. Garofalo, F., "Creep Rupture Behavior of Notched and Unnotched Specimens of Type 304, 316 and 321 Austenitic Stainless Steels," ASTM Proceedings, Vol. 59, pp. 957-972, 1959.

9. "Mechanical Properties Test Data for Structural Materials Quarterly Progress Report for Period Ending Jan. 31, 1978," ORNL-5380, Oak Ridge National Laboratory, March 1978. [Availability: USDOE, Technical Information Center].

THE CRBRP UPPER INTERNALS STRUCTURE

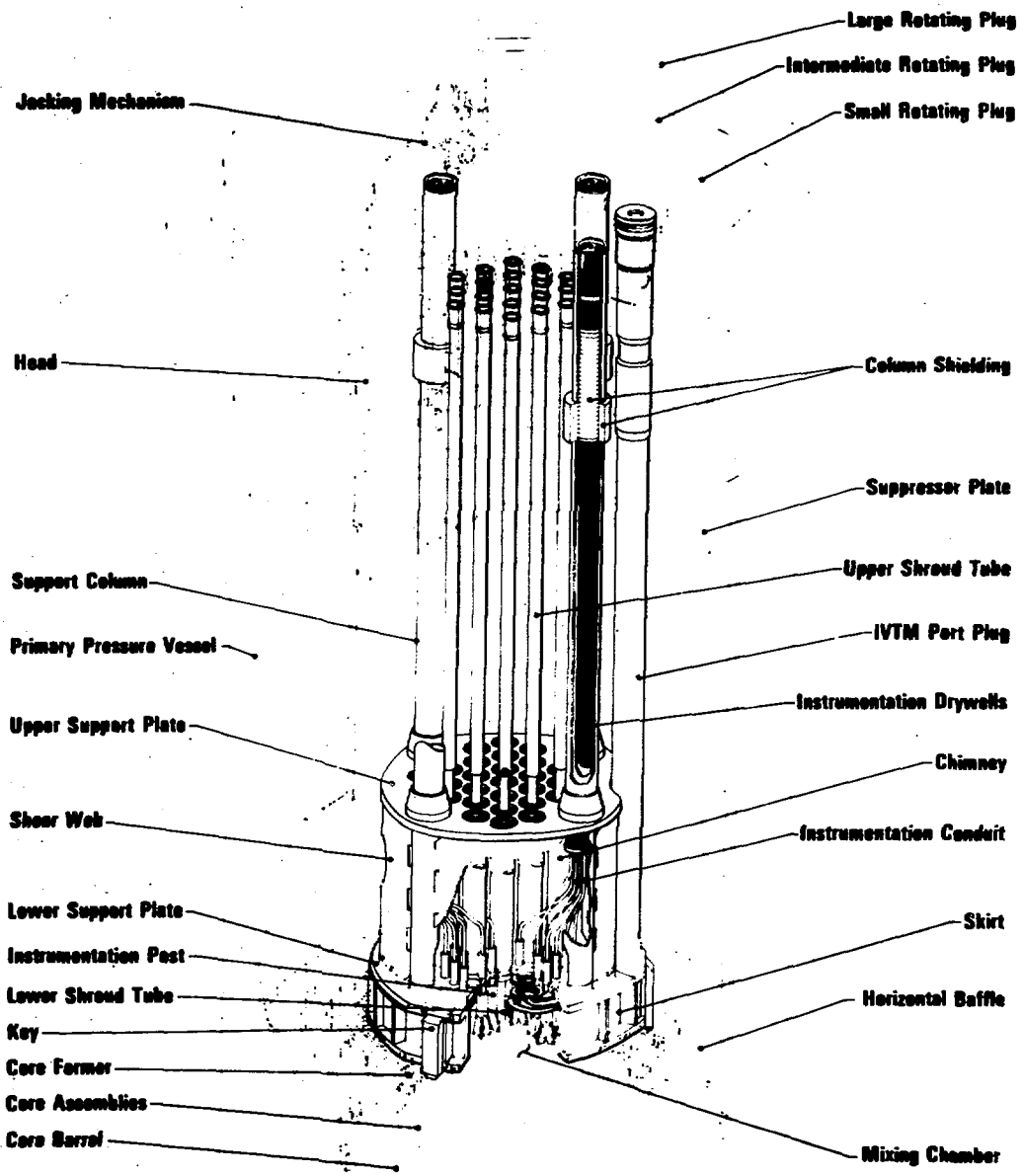

FIGURE 1

SEVERITY OF STRIPING IN UIS
RANGE OF FLUCTUATION °F

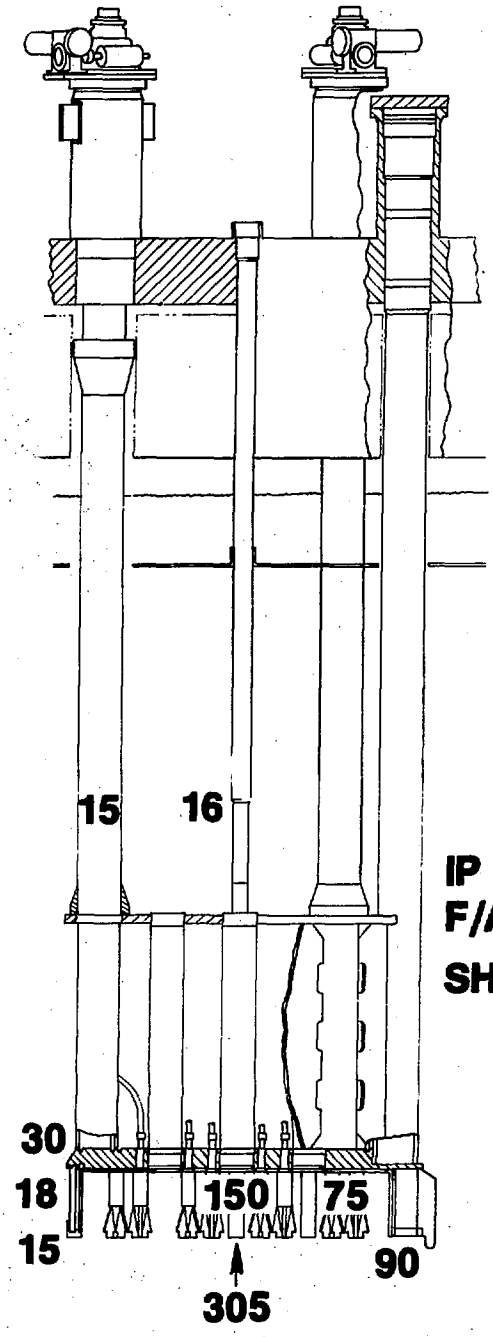

IP 271° NOMINAL 305° (2σ)
F/A -F/A 115° NOMINAL 150° (2σ)
SHROUD — 2σ (117°F)

UIS STEADY STATE TEMPERATURE (°F) DISTRIBUTION

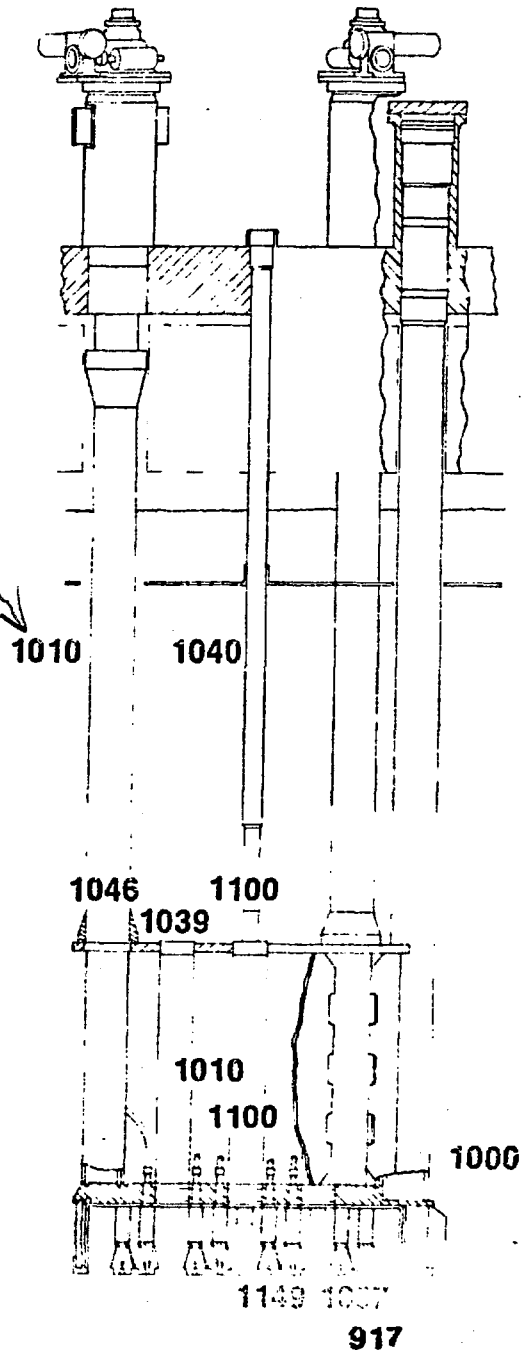

Type 11 Nos. Same size

1010.
1040
1046
1100
1039
1010
1100
1000
1149
1057
917

8081-15

FIGURE 3

CHIMNEY MIXED TEMPERATURES AT STEADY STATE CONDITIONS

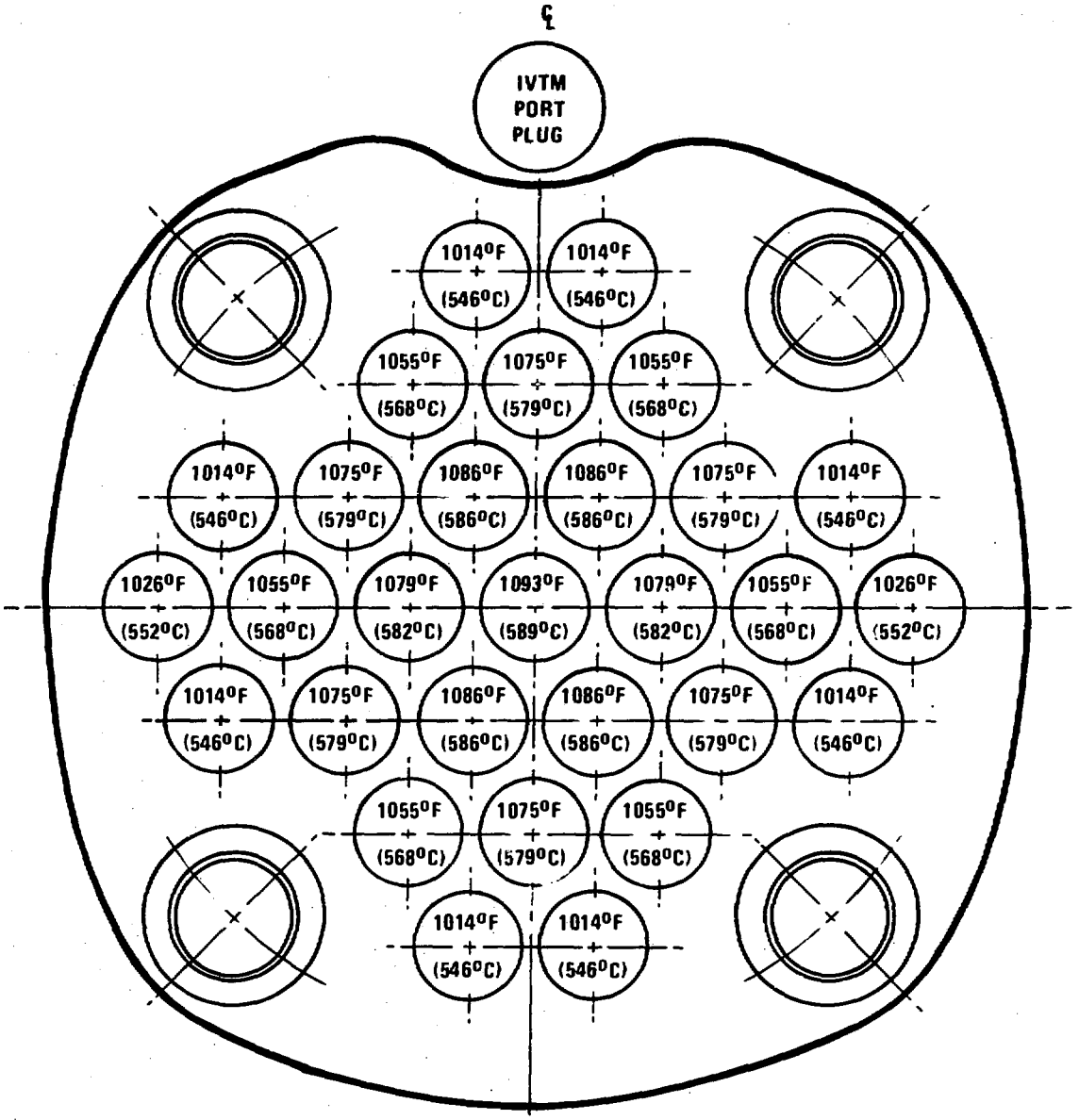

0847-4

FIGURE 4

FUEL ASSEMBLY EXIT TEMPERATURES FOR U-2 B, U-18, AND E-16 TRANSIENT EVENTS

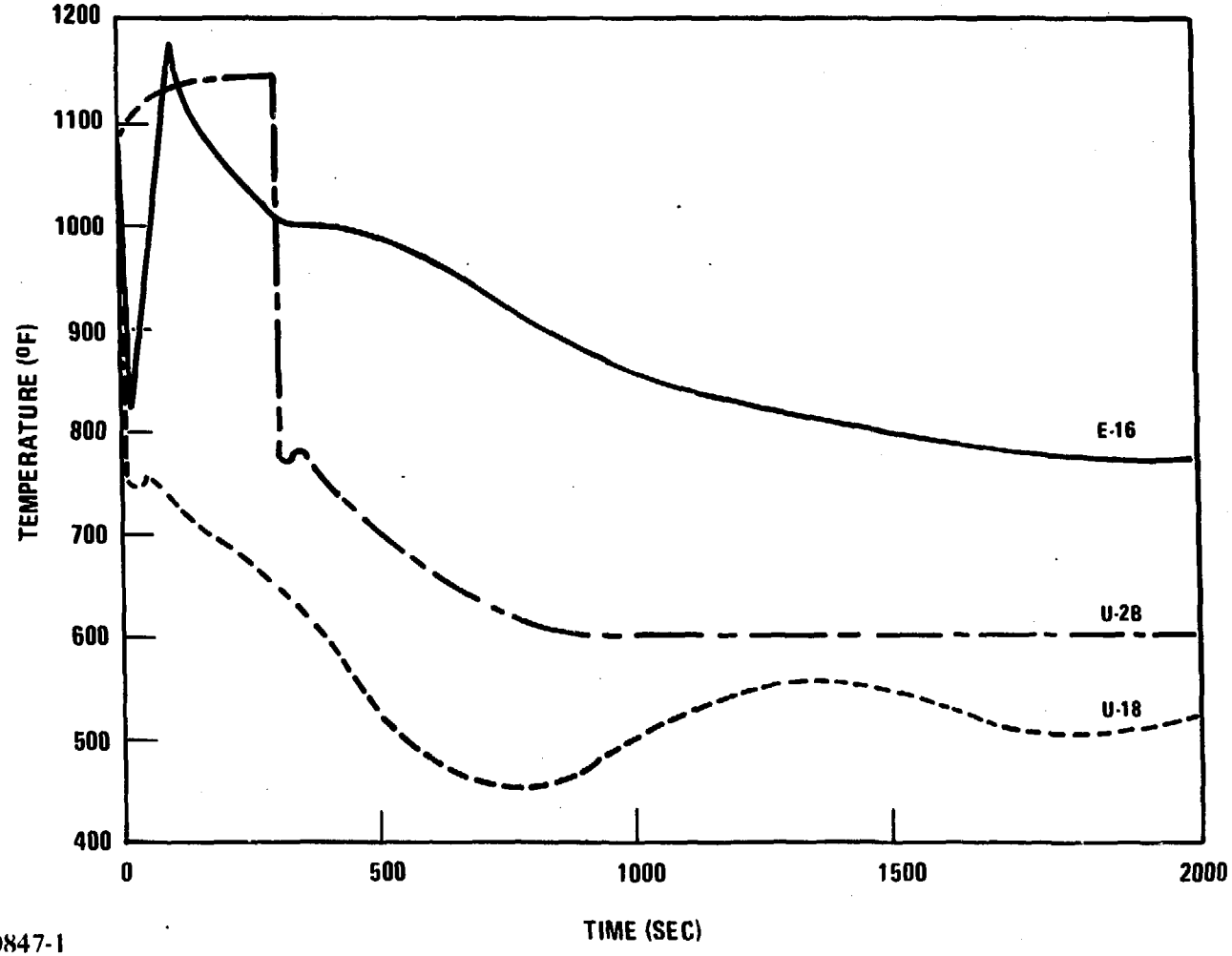

0847-1

FIGURE 5

DESIGN CURVES FOR HIGH CYCLE FATIGUE

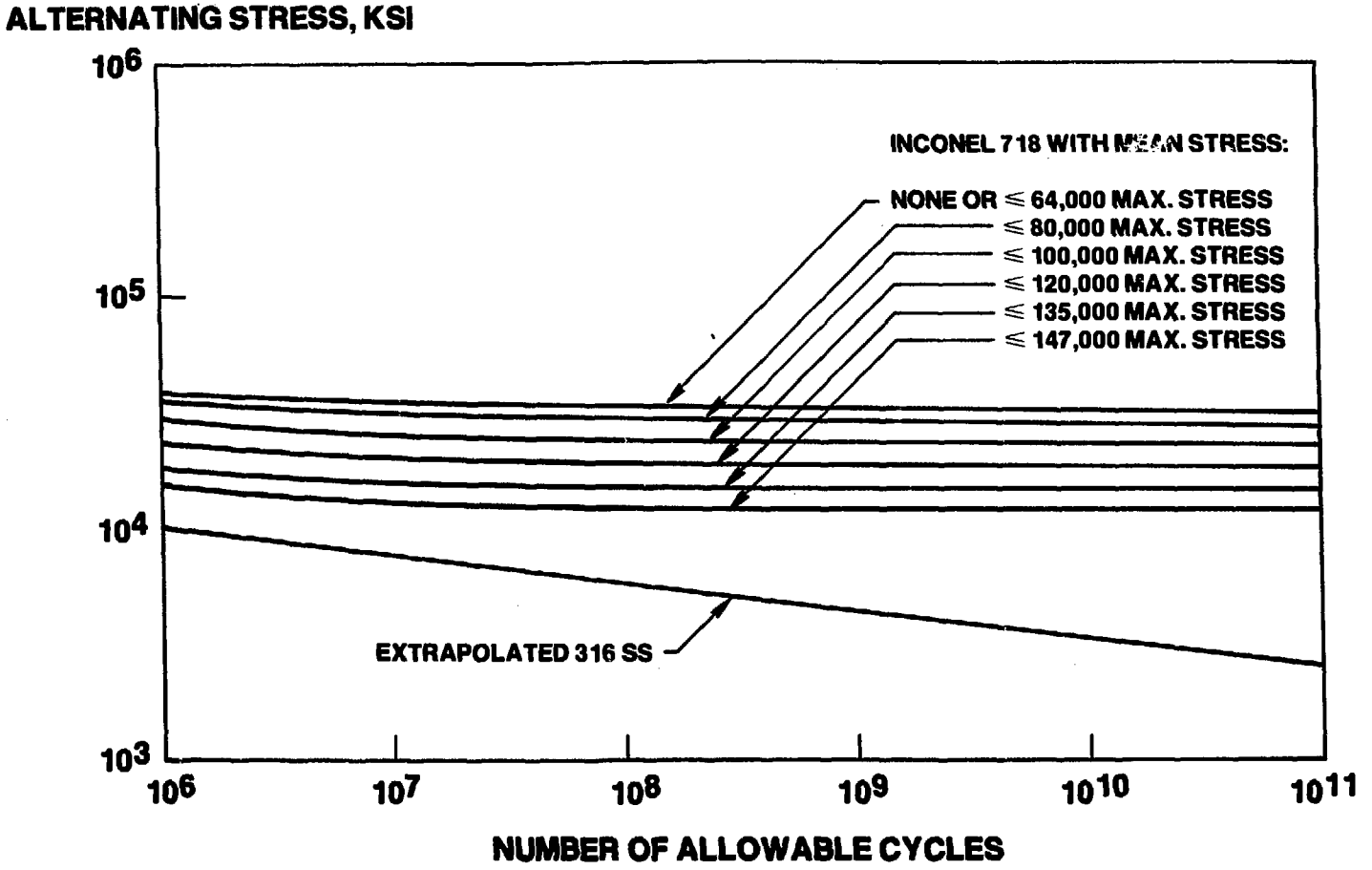

FIGURE 6

40%

CAPABILITY TO MEET REQ'TS FOR SINUSOIDAL STRIPING ON A 3/8 INCH SECTION

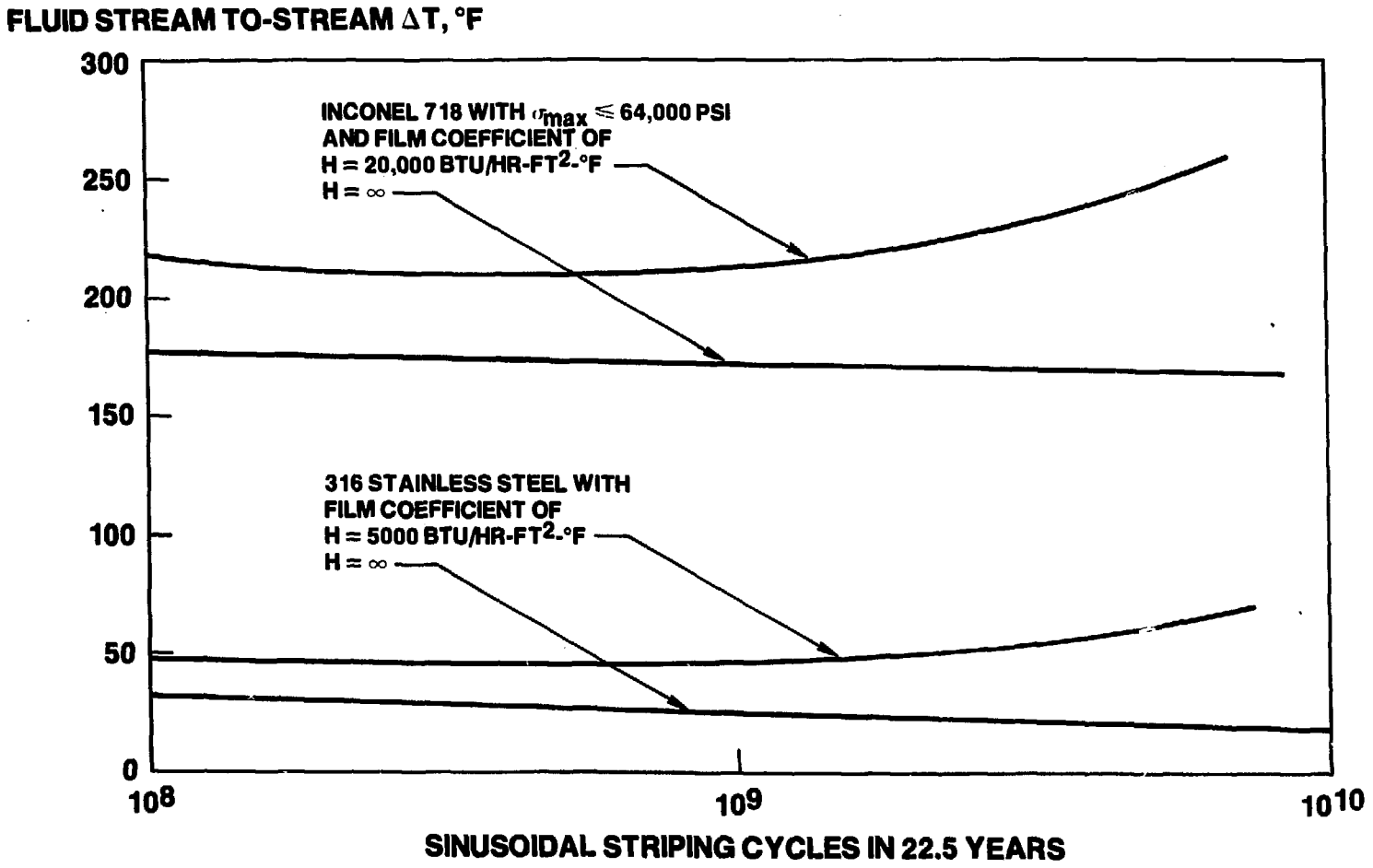

FIGURE 7

CREEP DAMAGE VERSUS HOLD-TIME TEMPERATURE FOR 316 STAINLESS STEEL IN SODIUM

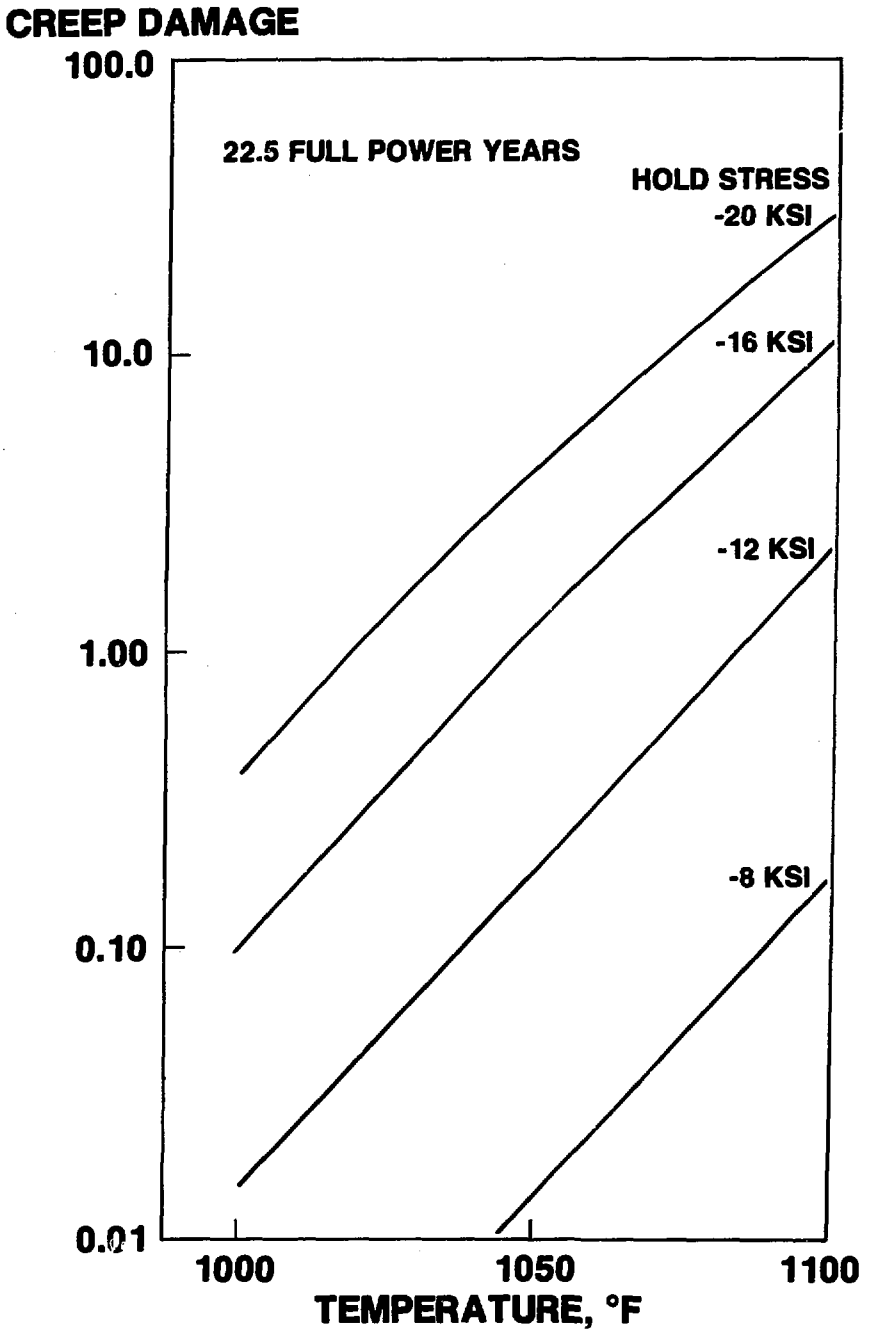

FIGURE 8

BI-LINEAR CONSTRUCTION TO OBTAIN THE INITIAL RESIDUAL STRESS AFTER DECAYING OF THE TRANSIENT

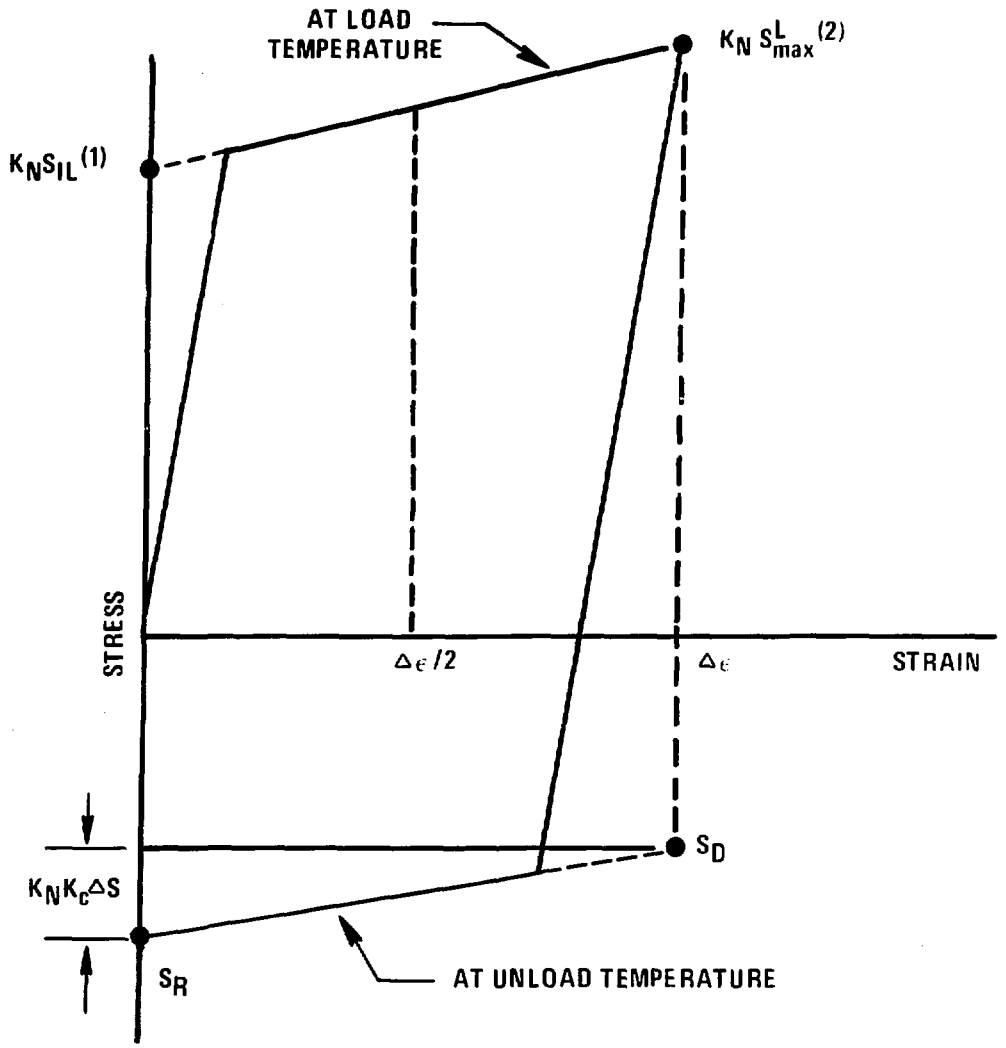

(1) S_{IU} IS THE SIMILAR VALUE (TO S_{IL}) FROM THE STRESS-STRAIN CURVE AT THE "UNLOAD" TEMPERATURE.

(2) S^U_{max} IS THE SIMILAR VALUE (TO S^L_{max}) FROM THE STRESS-STRAIN CURVE AT THE "UNLOAD" TEMPERATURE.

FIGURE 9

VARIATION OF DAMAGE WITH THICKNESS OF UNPROTECTED SECTIONS AT VARIOUS STEADY STATE TEMPERATURES

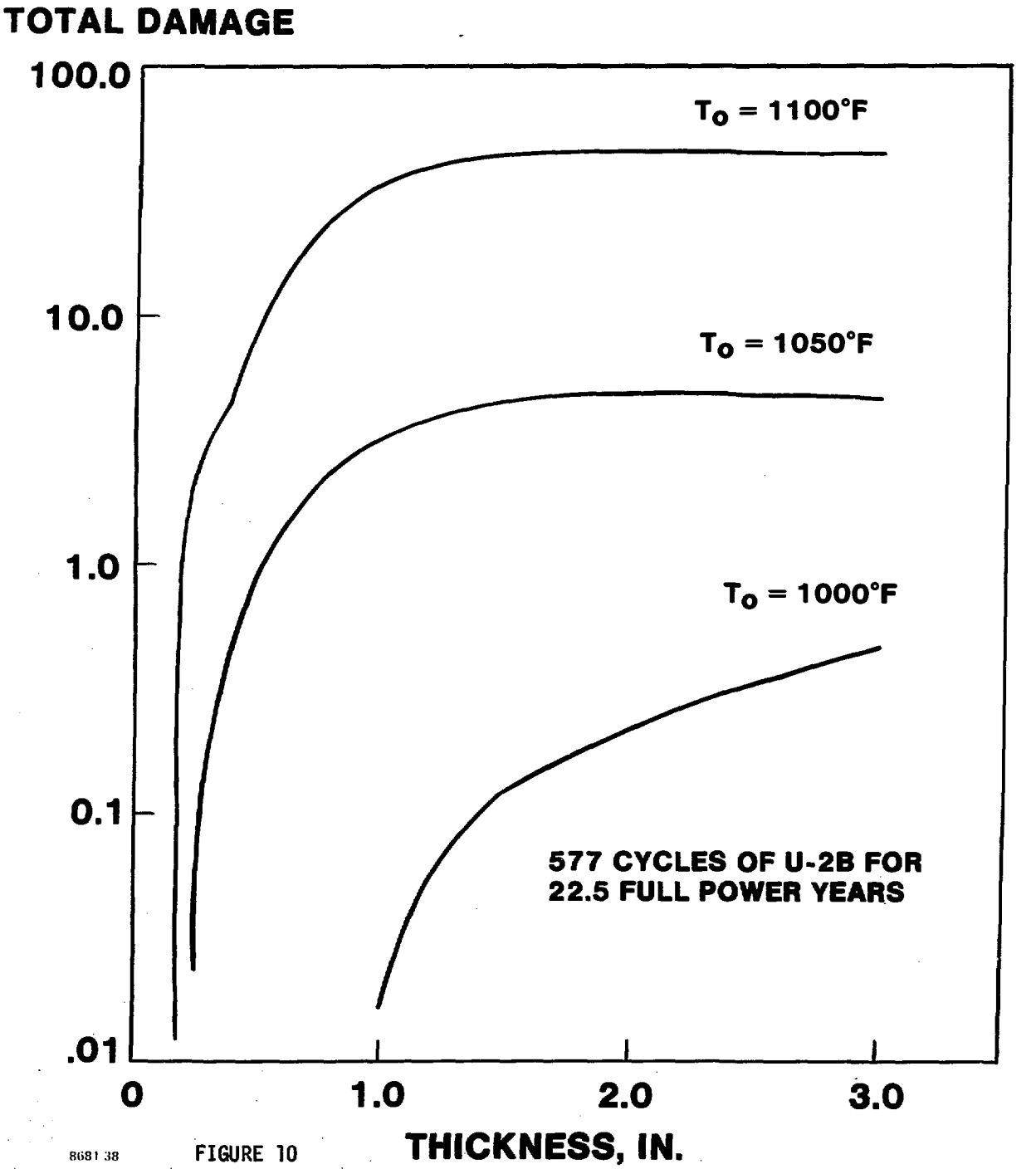

8681 38 FIGURE 10

EFFECT OF LINER THICKNESS ON TOTAL DAMAGE OF A 1.5 INCH THICK SECTION AT 1100°F

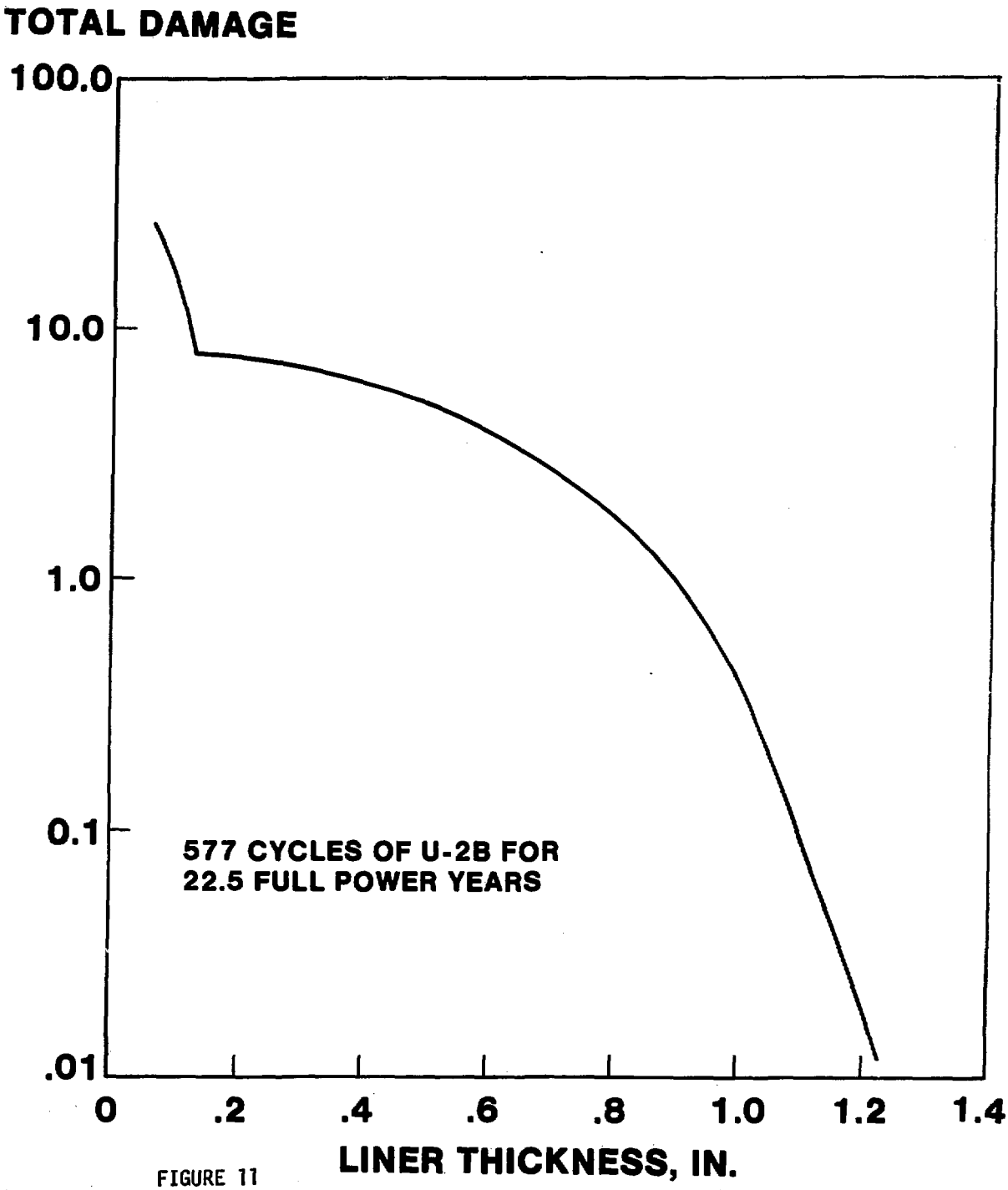

FIGURE 11

8681 39

THE UIS SEISMIC ANALYSIS MODEL

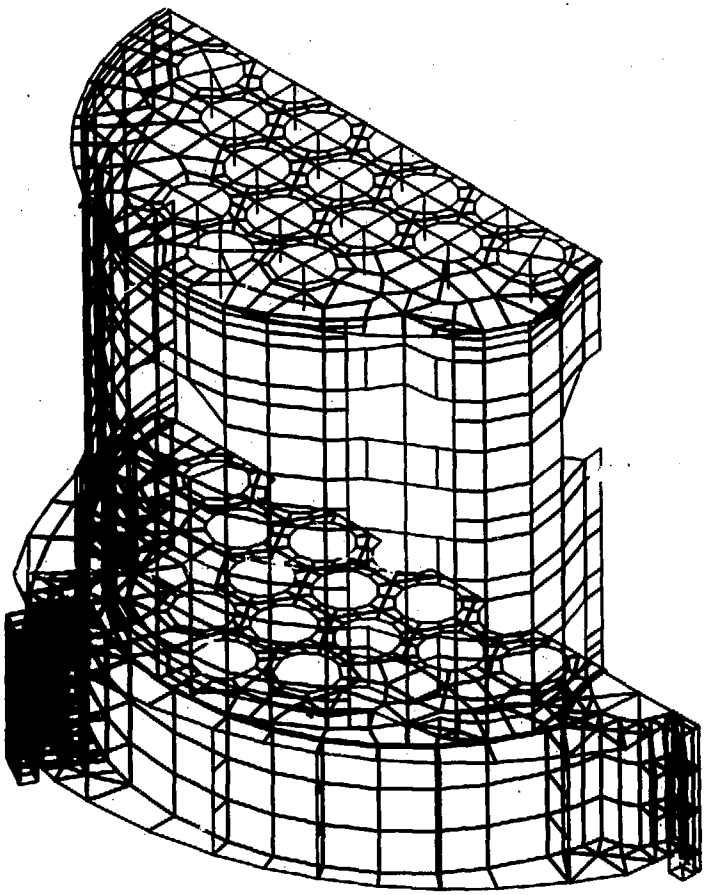

FIGURE 12

CRBRP UPPER INTERNALS STRUCTURE FINITE ELEMENT MODELS

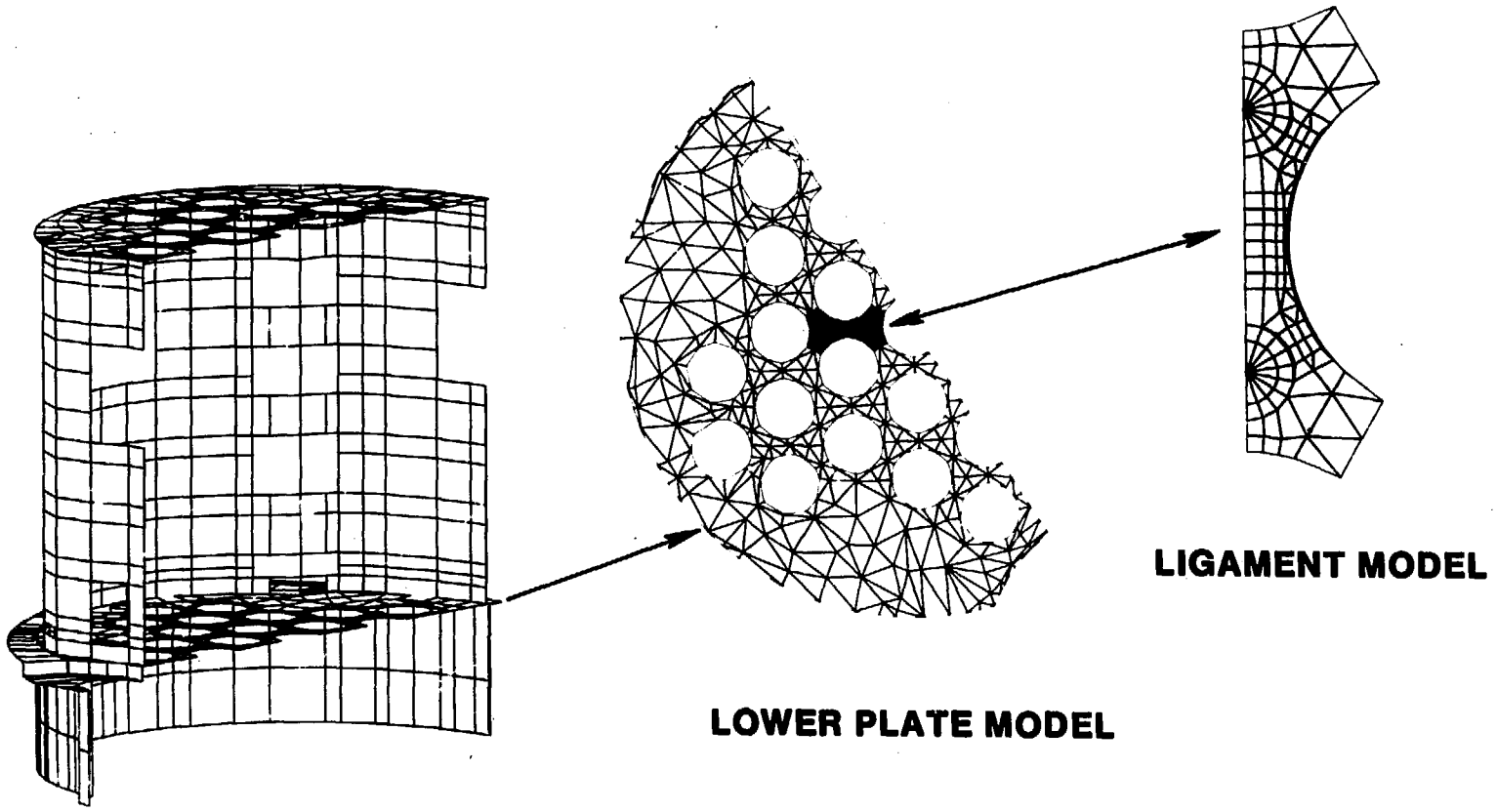

FIGURE 13

LIGAMENT RESPONSE AT BOTTOM CORNER OF MINIMUM SECTION

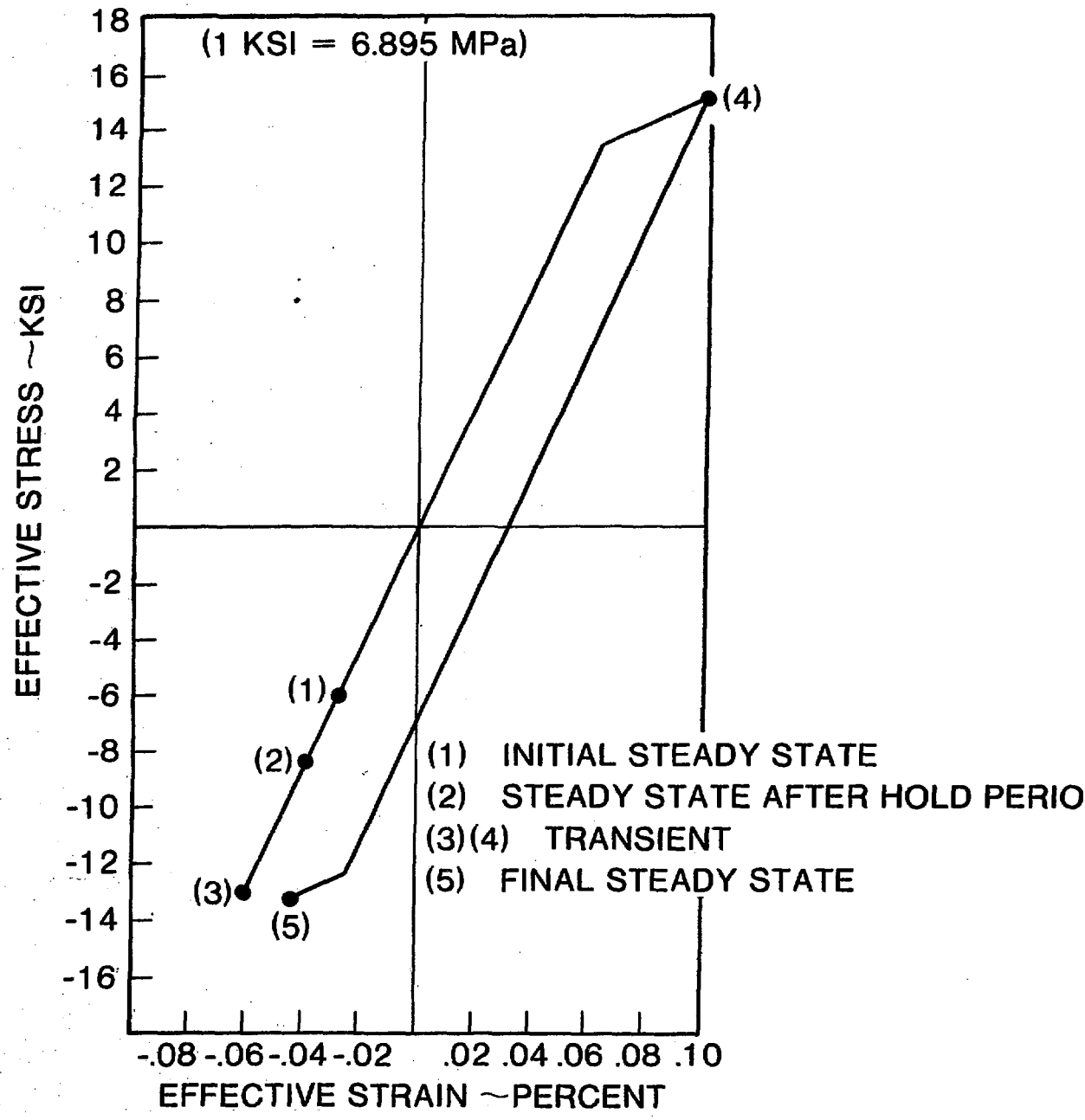

FIGURE 14